Journal of Biomedical Informatics 58 (2015) 96–103

Contents lists available at ScienceDirect

Journal of Biomedical Informatics

journal homepage: www.elsevier.com/locate/yjbin

Detecting glaucomatous change in visual fields: Analysis with an optimization framework

Siamak Yousefi [a], Michael H. Goldbaum [a], Ehsan S. Varnousfaderani [a], Akram Belghith [a], Tzyy-Ping Jung [b], Felipe A. Medeiros [a], Linda M. Zangwill [a], Robert N. Weinreb [a], Jeffrey M. Liebmann [c], Christopher A. Girkin [d], Christopher Bowd [a,*]

[a] Hamilton Glaucoma Center and the Department of Ophthalmology, University of California San Diego, La Jolla, CA, USA
[b] Institute for Neural Computation and Institute of Engineering in Medicine, University of California San Diego, La Jolla, CA, USA
[c] Department of Ophthalmology, Columbia University, New York, NY, USA
[d] Department of Ophthalmology, University of Alabama, Birmingham, AL, USA

ARTICLE INFO

Article history:
Received 2 April 2015
Revised 15 September 2015
Accepted 27 September 2015
Available online 9 October 2015

Keywords:
Data mining
Change detection
Computational modeling
Glaucoma
Progression
Visual field
Standard automated perimetry

ABSTRACT

Detecting glaucomatous progression is an important aspect of glaucoma management. The assessment of longitudinal series of visual fields, measured using Standard Automated Perimetry (SAP), is considered the reference standard for this effort. We seek efficient techniques for determining progression from longitudinal visual fields by formulating the problem as an optimization framework, learned from a population of glaucoma data. The longitudinal data from each patient's eye were used in a convex optimization framework to find a vector that is representative of the progression direction of the sample population, as a whole. Post-hoc analysis of longitudinal visual fields across the derived vector led to optimal progression (change) detection. The proposed method was compared to recently described progression detection methods and to linear regression of instrument-defined global indices, and showed slightly higher sensitivities at the highest specificities than other methods (a clinically desirable result). The proposed approach is simpler, faster, and more efficient for detecting glaucomatous changes, compared to our previously proposed machine learning-based methods, although it provides somewhat less information. This approach has potential application in glaucoma clinics for patient monitoring and in research centers for classification of study participants.

1. Introduction

Glaucoma, a group of optic neuropathies, is one of the two leading causes of preventable blindness and affects more than 60 million individuals worldwide [1,2]. Glaucoma causes morphological changes of the optic disk accompanied by visual field damage that is slowly progressing, with a time course of several years. The patient often is not aware of visual field loss in the early stages of the disease [1,2]. Detecting structural and functional changes associated with glaucoma is important to the physician who must decide whether the current therapy is preventing the progression of the disease or whether some more invasive treatment (e.g., surgery) is necessary. Determining whether visual field defects have progressed in individual patients remains one of the most challenging aspects of glaucoma management.

Standard Automated Perimetry (SAP) is an established visual function test for identifying glaucoma and assessing its severity. Current SAP software measures the retinal sensitivity to light at 52 different test points (for 24-2 stimuli, with a visible range from 0 dB to approximately 40 dB) as projected onto the retina from the visual field. Status of test locations (e.g., within normal limits or outside of normal limits) is determined by statistical comparison with the instrument's normative database composed of age normalized SAP results [3]. Fig. 1 shows how the visual field is collected from the instrument and a sample visual field test and data vector (52-dimensional). To detect change, i.e., glaucomatous progression, eye experts subjectively monitor a sequence of SAP tests. This subjectivity often results in biased or inconsistent decisions [4]. We seek to make the process more objective. Computational methods are desirable because these methods produce objective outcomes and overcome potentially biased or inconsistent strategies.

Several methods have been developed to identify change in glaucomatous visual fields over time. Some of these methods are

* Corresponding author.
E-mail address: cbowd@ucsd.edu (C. Bowd).

http://dx.doi.org/10.1016/j.jbi.2015.09.019
1532-0464/

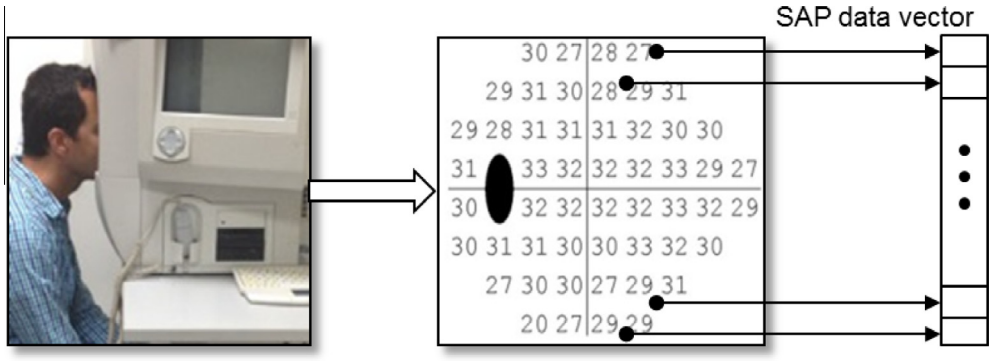

Fig. 1. SAP visual field collection, a sample pattern, and data vector.

event-based (in which a follow-up examination is compared to baseline examinations, with an event, e.g., progression or no progression, assigned if change is greater than predetermined criteria) and some are trend-based (in which the rate of change is estimated based on regression analysis of a sequence of visual field examinations). Because the currently proposed method is trend-based, we describe seven other trend-based methods. (1) Ordinary least square regression (OLSR) of the commercially available SAP software parameters mean deviation (MD), that reflects global change (whereas glaucoma changes often are localized) [5] and (2) OLSR of Visual Field Index (VFI) that is calculated based on a weighted distribution of values from each visual field point and hence is correlated with patient visual function [6,7]. Both methods one and two are based on instrument-generated global indices.

(3) Point-wise linear regression (PLR), that tracks change at each individual visual field location over the entire follow-up duration. For PLR, progression is arbitrarily defined based on a fixed number of changing test locations. PLR is calculated in the commercially available Progressor software [8]. PLR does not provide a strictly defined significance value for the severity of deterioration of the whole visual field, which makes it difficult to interpret [9]. (4) Permutation Analysis of PLR (PoPLR) is an individualized analysis that uses a p value combination function and permutation analysis to detect glaucomatous change [9]. PoPLR requires a baseline exam and at least six independent sequential follow-up exams to generate greater than 1000 permutations, required to calculate a robust rate of change estimate. The application of PLR and PoPLR to other glaucoma-related measurements (e.g., retinal nerve fiber layer thickness measurement) has not yet been reported. Both PLR and PoPLR are individualized methods; the decision regarding progression is made based on individual patient data and not based on population data.

(5) Analysis with Non-Stationary Weibull Error Regression and Spatial Enhancement (ANSWERS), relies on a mixture of Weibull distributions to model visual field variability and a Bayesian method to aggregate the spatial correlation of local measurements to confirm repeatable defects in the same or adjacent locations in follow-up examinations [10]. ANSWERS was designed specifically to detect progression in SAP visual fields. The application of ANSWERS to other glaucoma-related measurements has not yet been reported.

Recent advances in machine learning techniques provide new approaches for glaucoma-related diagnosis and progression detection based on learning from a pool of data [11–15]. (6) Variational Bayesian independent component analysis mixture model (VIM) for glaucoma defect pattern identification and progression detection is a machine learning classification-based approach developed by our group [16–18]. (7) Gaussian Mixture Model with Expectation Maximization (GEM), another machine learning-based approach, recently was introduced by our group and was successfully applied to visual field data to identify glaucoma-related defect patterns and to detect progression [19]. The initial creation of an environment using these machine learning approaches for progression detection is computationally and algorithmically complex.

All of the above methods are trend-based approaches. Methods one and two also provide the rate of progression, while methods three to seven simply indicate whether the eye is progressing without any information on the rate of progression.

Guided Progression Analysis (GPA), an instrument-generated parameter, is an example of an event-based analysis [20]. GPA analyzes the test point by test point pattern deviation of a sequence of visual fields to identify glaucomatous progression. GPA requires two baseline and three follow-up exams to assign a result of "likely progression".

In this paper, we propose an approach for glaucoma change detection using an optimization framework (abbreviated CDOF). This approach is based on learning from a population of glaucoma data and can be applied to visual fields for detecting glaucomatous progression with the capability of providing an estimate of the rate of progression. Our method was designed to be robust, in that it can be applied to estimate the rate of change in any multidimensional data, including structural imaging tests. We will show that the proposed framework requires only longitudinal data for training compared to our previously proposed machine learning-based models, VIM and GEM, that require both cross-sectional and longitudinal data [17,21]. We then demonstrate that the proposed framework is algorithmically and computationally less complex than VIM and GEM.

Table 1 provides a comparison between the different glaucoma progression detection methods described above. The information provided in the table follows:

(1) Is the method trend- or event-based? Trend-based methods typically rely on linear regression of an independent variable, and theoretically two visits are enough to detect change based on these methods; however, in practice far more than two visits are necessary for these methods to provide a robust estimation, due to longitudinal test–retest variability [22].
(2) Does the method make use of individual or population-based data? Some of the population-based methods need a large group of subjects and an environment for detecting change (e.g., methods five through eight). GPA, PLR, and PoPLR methods do not require any additional information other than longitudinal visual fields of the test eye to detect progression or glaucoma-related change. These individual-

Table 1
Comparison of different glaucoma progression detection methods.

Method	Trend- or event-based	Individualized or population-based	Local or global analysis	Provides rate of change
OLSR of MD	Trend-based	Population-based	Global analysis	Yes
OLSR of VFI	Trend-based	Population-based	Global analysis	Yes
PLR	Trend-based	Individualized	Local analysis	No
PoPLR	Trend-based	Individualized	Local analysis	No
ANSWERS	Trend-based	Population-based	Local analysis	No
VIM	Trend-based	Population-based	Local analysis	No
GEM	Trend-based	Population-based	Local analysis	No
CDOF	Trend-based	Population-based	Local analysis	Yes
GPA	Event-based	Individualized	Local analysis	No

based methods generally are less complex than population-based methods because they don't require analyzing a population of eyes for creating an environment (calculating model parameters) for progression detection.

(3) Is the analysis based on global or local measurements? OLSR of MD and VFI are considered global methods because MD and VFI are global indices. Local methods either analyze each individual visual field test location on a point by point basis, e.g., GPA, PLR, and PoPLR; or they analyze a subset of visual field test locations, e.g., ANSWERS, VIM, GEM and CDOF. Local methods are theoretically more accurate than global methods, because they allow the user to exclude uninformative test locations.

(4) Does the method provide rate-of-change information? Having access to the progression rate offers eye specialists additional relevant information for disease management.

2. Method

2.1. Participants

Study participants were selected from two University of California at San Diego (UCSD)-based studies; the Diagnostic Innovations in Glaucoma Study (DIGS) and the African Descent and Glaucoma Evaluation Study (ADAGES, a multicenter study). Both studies adhered to the tenets of the Declaration of Helsinki and to the Health Insurance Portability and Accountability Act, and all participants provided written informed consent. SAP testing was performed using the 24-2 Swedish Interactive Thresholding Algorithm (SITA), and unreliable tests (>33% fixation losses or false-negative results or >15% false-positive results) were excluded. Trained reviewers from the UCSD-based Visual Field Assessment Center (VisFACt) assessed all visual field tests studied for any apparent artifacts (e.g., lid or rim artifacts, signs of fatigue).

2.2. Datasets

Two different longitudinal datasets were employed. The first dataset included 91 eyes from 48 study participants with repeatable glaucomatous SAP defects at baseline (defined as pattern standard deviation (PSD) $\leqslant$ 0.05 or a glaucoma hemifield test outside of normal limits [23]). Each study eye was tested once a week for about 5 weeks, resulting in the collection of 421 SAP visual field measurements. Because glaucoma develops over years and not weeks, we assumed any changes during this short follow-up duration likely would be due to noise and other sources of variability. This dataset simulates stable eyes with glaucoma followed for years, constitutes our control patients, and is called the *stable group*.

The second dataset included 83 eyes from 74 study participants with known progressive glaucomatous optic neuropathy that was defined as an apparent decrease in the neuroretinal rim width, or the appearance of a new or enlarged retinal nerve fiber layer defect in paired longitudinal stereoscopic images by observers masked to patient identification and diagnosis. This assessment was independent of any visual field changes in the classification step to avoid any bias in the evaluation of the proposed method that uses visual field measurements to detect progression. A total of 1,161 SAP visual field measurement visits were available from this group. This dataset constitutes our *progressed group*. In Table 2 we have provided the demographic information of the participants in the *stable* and *progressed* groups. A decrease in MD indicates increased disease severity; an increase in PSD corresponds to an increased disease severity.

2.3. Pipeline

Fig. 2 shows the entire pipeline for glaucoma change detection. Step one includes visual field preprocessing to generate SAP feature vectors for the optimization framework. As shown in Fig. 3, for each eye, we sort all longitudinal SAP data vectors in time and we then compute the difference between each SAP data vector and its follow-up. Doing so, we obtain a longitudinal time series of feature vectors for each eye.

If the visual field abnormality (defined above) progresses over time, then the magnitude of SAP feature vectors becomes increasingly large. Therefore, in step two, the problem of detecting change in the visual field of an eye over time can be framed as the problem

Table 2
Demographic information of study eyes.

Parameter	Stable	Progressed by photo	*p*-Value
Number of eyes	91	83	–
Number of subjects	48	74	–
Mean number of visual field follow-up (S.D.)	4.7 (0.8)	14 (4.8)	<0.01
Months of follow-up (S.D.)	1.1 (0.2)	109.2 (26.4)	<0.01
Age at baseline in years (S.D.)	70.9 (9.5)	62.5 (12.4)	<0.01
Percent male	55	48	0.18
Baseline MD in dB (S.D.)	−7.4 (8.2)	−4.4 (5.8)	<0.01
Baseline PSD in dB (S.D.)	6 (4.2)	5 (4.2)	0.12

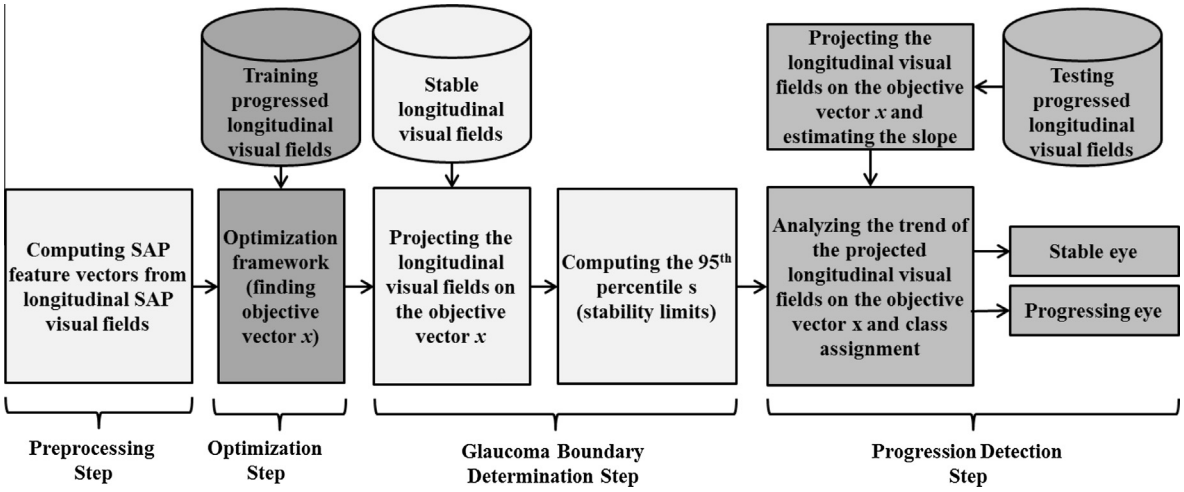

Fig. 2. Pipeline for progression detection using optimization framework.

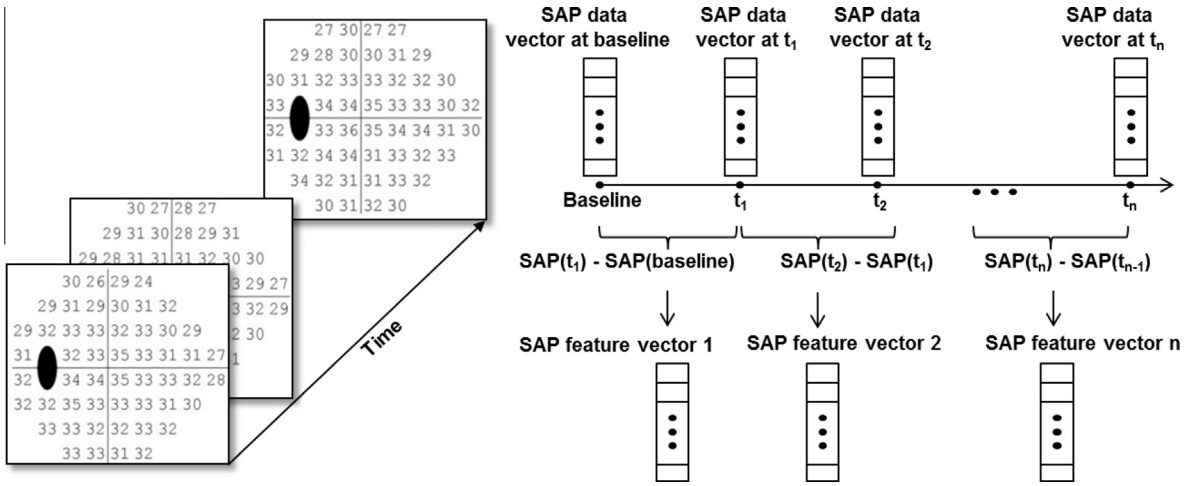

Fig. 3. Preprocessing: longitudinal SAP visual fields and feature vector creation.

of detecting the change in magnitude of the SAP feature vectors over time. We seek a vector (direction) where the amount of change (for all feature vectors from progressed eyes over time) along that vector is maximal. This can be formulated as an optimization framework to find the optimal vector (direction) for detecting change in visual field (loss) over time. Fig. 3 shows the process of feature vector creation (i.e., preprocessing), schematically.

Essentially, step two is a combination of classification and optimization. In this step, we first find the parameters of the optimization framework based on the SAP feature vectors of 80% of the eyes in the progressed group and then test the optimization framework model against the remaining 20% of the eyes in the progressed group (no overlap in training data, i.e., five-fold cross-validation). We calculate the SAP feature vectors for all eyes in the training subset. Mathematically, finding a vector (direction) in 52-dimensional space that maximizes the likelihood of change detection is equivalent to minimizing the inner product of all SAP feature vectors (calculated from visual fields in the training group) and the objective vector (direction).

This vector (direction) constitutes the objective function of the optimization framework. The optimization framework is solved on a unit hypersphere (isoseverity surface) because we seek only the direction of the objective vector and not its magnitude (glaucoma severity).

Hence, we can formulate the problem of finding the optimal direction for detecting change as:

$$\begin{aligned} &\textit{minimize} \quad \sum_{i=1}^{n} q_i^T x \\ &\textit{subject to} \quad x^T P x - 1 = 0 \end{aligned} \tag{1}$$

where x is the objective vector (direction, of size 52×1), q_i is a SAP feature vector coefficient (size 52×1) (difference of visual fields at t_j and t_{j+1}), n is the number of feature vector coefficients (number of all SAP feature vectors from all eyes in the training group), P is the identity matrix of size 52×52, and 1 and 0 are scalar values. The constraint forces the objective vector x to terminate on the surface of the unit hypersphere. This framework is convex because the objective function is linear and the equality constraint has a quadratic form [24]. Therefore, we minimize a linear objective function over a convex set, a hypersphere including the feasible set of vectors. More specifically, this framework is a quadratically constrained quadratic program (QCQP) [24] and has a global minimum that can be solved efficiently using convex optimization solvers. Solving the optimization framework above provides us the optimal vector or direction for analyzing glaucoma change in the original SAP visual field space.

The optimization framework was trained five times on the training data, each time excluding one of the partitions for testing. Therefore, we computed five different objective vectors based on five different training datasets. We used CVX, the Matlab software for disciplined convex programming for constructing and solving

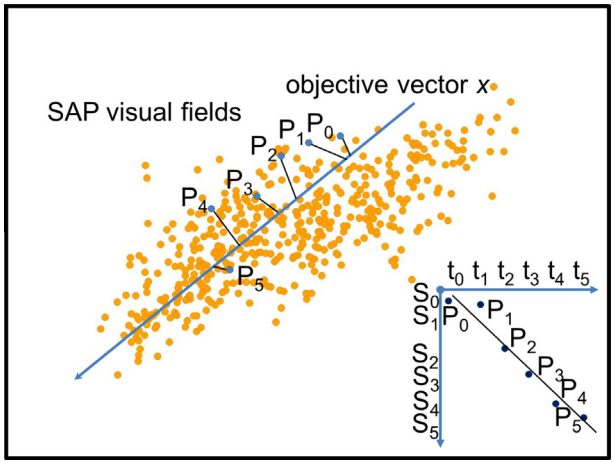

Fig. 4. Glaucoma boundary limit specification. Projecting the visual field data vectors on the objective vector x and estimating the slope using linear regression. P_0 to P_5 indicate six longitudinal visual field data vectors for an eye. S_0 to S_5 indicate the projected values on the objective vector x.

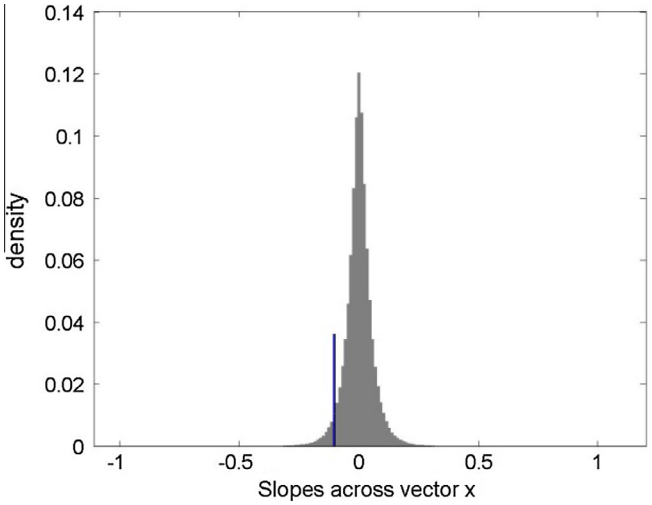

Fig. 5. Distribution of the linear regression slopes of the projected visual fields data vectors of all eyes in the stable group on the objective vector x. The blue line indicates the left tail 95th percentile. (For interpretation of the references to color in this figure legend, the reader is referred to the web version of this article.)

the proposed convex program [25,26]. The optimization step results in the objective vector x, and analyzing the visual fields across that vector maximizes the likelihood of detecting change (progression).

In step three, we calculate the glaucoma boundary limits as shown in Fig. 4. To this purpose, we use the stable dataset (where each eye has 5 visits over a short duration). First, to simulate a stable eye with 10 visits, SAP longitudinal data vectors of each eye in the stable dataset were randomly resampled 1000 times with replacement using the bootstrap method, to mimic the average number of visits in the eyes from the progressed dataset. The longitudinal sequence of visual field data vectors of each stable eye were projected onto the identified objective vector x and the rate of progression of each visual field data vector was calculated using linear regression as shown in Fig. 4.

Then the 95th percentiles towards the direction of deterioration for objective vector x was calculated from the histogram of the slopes. Because eyes in the *stable group* presumably showed no disease related progression, the variability in this group was used to define the progression limits. This procedure was repeated five times (for five-folds), each time using the identified objective vector x for that fold. The outcome of the glaucoma boundary determination step is five glaucoma boundaries (95th percentiles) for each classification fold.

Step four is the progression detection step. We used the previously described Progression of Patterns (POP) [17] along objective vector x for detecting change (progression). Specifically, each visit (among a series of longitudinal visual field data vectors) of each eye in the test fold of the progressed group was projected onto the objective vector x, corresponding to its training fold. The rate of progression (slope) of the longitudinal sequence of visual field data vectors along the objective vector x was estimated using linear regression. The test eye was classified as progressed when the rate of progression exceeded the 95th percentile progression limit developed on the eyes with simulated stability; otherwise, the eye was classified as non-progressed.

To compare our method against linear regression of MD and VFI, a similar procedure was performed to define the limits of stability to detect progression using those global metrics. For PLR and PoPLR, we followed the same procedure as previously described [8,9].

3. Results and discussion

Fig. 5 shows the distribution of the slopes of the projection magnitudes of all visual field data vectors in the stable group along objective vector x (from one fold). The left tail of the 95th percentile limit is shown as a blue line. For a test eye, if its slope exceeded this limit, the eye was classified as progressed.

Fig. 6 shows progression detection in two example eyes. The orange circles represent the magnitude of the projected visual field data vector (severity) along objective vector x. The blue line indicates the slope of the orange circles approximated using a linear regression. The gray line indicates the glaucoma boundary limit across the objective vector x (95th percentile of the stable eyes across that vector). If the estimated slope falls below the gray line (progression zone), then the eye is classified as progressed; otherwise, the eye is classified as non-progressed. Therefore, the study eye in Fig. 6 (left panel) is detected as progressed and the study eye in Fig. 6 (right panel) is detected as non-progressed. The rate of progression is shown graphically. Visual field loss of the eye in the left panel is faster than the eye in the right panel.

Table 3 shows the progression detection sensitivities of CDOF, VIM, GEM, PoPLR, PLR, linear regression of MD, and linear regression of VFI at various specificities. Because we used two independent datasets in our analysis to define glaucoma boundary limits and to detect progression, we were unable to obtain continuous specificity and sensitivity for PoPLR and PLR. Therefore, we have listed sensitivity and specificity trade-offs at eight discrete points along the ROC curve shown in Fig. 7.

Fig. 7 shows the ROC curves between 85% and 100% specificities for CDOF, VIM, GEM, linear regression of MD and linear regression of VFI and the discrete sensitivity–specificity responses of PoPLR and PLR methods. It can be observed that the performance of CDOF, VIM, GEM, PoPLR, and PLR are similar and are significantly better than linear regression of MD and linear regression of VFI. At higher specificities, CDOF slightly outperforms VIM, GEM, PoPLR and PLR methods however, as Table 3 shows, differences are not statistically significant.

To employ our algorithm in a clinical setting, we will identify the objective vector x from all data in the progressed group, compute the glaucoma boundary limits and save all of the parameters. Clinicians and researchers will be able to feed the longitudinal

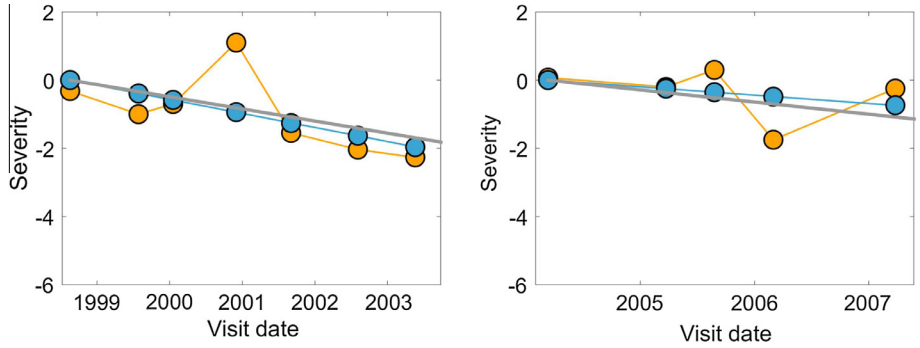

Fig. 6. Progression detection by the proposed optimization framework in two sample eyes. The gray line indicates the 95th percentile limit. The orange circles represent the actual projected visual field values on objective vector *x*, and the blue circles are linear regression approximations of the orange circles. The eye in the left panel is classified as progressed and the eye in the right panel is classified as non-progressed.

Table 3
Progression detection sensitivities (and corresponding confidence intervals) of CDOF, VIM, GEM, PLR, PoPLR, MD and VFI at various specificities (Bold values indicate best performing method at each listed specificity).

Specificity (%)	Sensitivity [confidence interval]						
	CDOF	VIM	GEM	PoPLR	PLR	MD	VFI
100	**8.7** [1.4,14]	2.4 [0.0,5.8]	4.8 [0.0,9.2]	6.1 [0.0,10.8]	–	0 [0.0,1.0]	0 [0.0,0.6]
99	**40.0** [24.3,46.1]	26.5 [13.6,33.0]	30.1 [16.4,36.6]	28.0 [14.8,34.5]	31.3 [17.3,37.7]	4.8 [0.0,9.0]	2.4 [0.0,5.8]
97	**47.5** [30.6,53]	44.6 [28.1,50.3]	42.2 [26.1,48.1]	31.7 [17.6,38.2]	–	15.4 [5.6,21.6]	8.3 [1.1,13.6]
96	**50.0** [32.7,55.3]	47.0 [30.1,52.5]	43.4 [27.1,49.2]	–	42.2 [26.1,48.1]	15.5 [5.6,21.6]	10.7 [2.5,16.3]
95	50.0 [32.6,55.2]	48.2 [31.1,53.6]	**50.6** [33.2,55.8]	41.5 [25.5,47.4]	44.6 [28.1,50.3]	16.7 [6.4,22.9]	14.3 [4.8,20.3]
93	52.5 [34.8,57.5]	53.1 [35.3,58.0]	**56.6** [38.5,61.6]	54.9 [36.9,59.6]	–	22.6 [10.7,29.1]	21.4 [9.8,27.8]
89	58.7 [40.3,63.5]	55.4 [37.3,60.1]	59.0 [40.6,63.3]	**61.0** [42.3,65.0]	–	32.1 [18.0,38.6]	29.8 [16.1,36.2]
87	61.2 [42.5,65.2]	59.0 [40.6,63.3]	60.2 [41.7,64.3]	**63.4** [44.5,67.1]	–	34.5 [19.9,40.9]	34.5 [19.8,40.9]

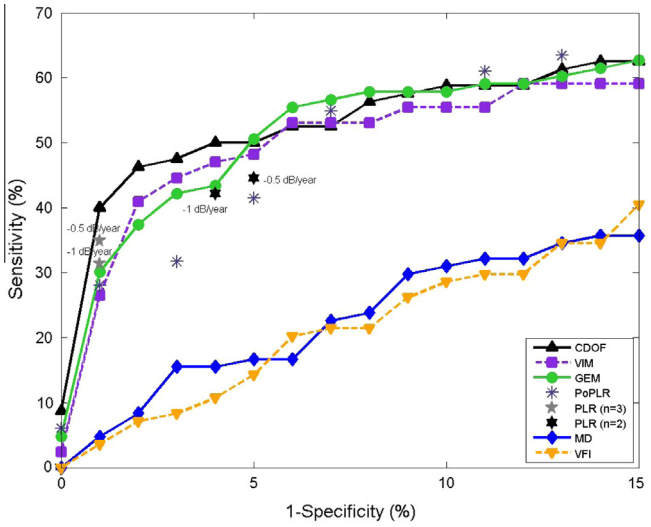

Fig. 7. Partial ROC curve showing sensitivity versus 1-specificity of CDOF, VIM, GEM, PoPLR, PLR (based on two significant deteriorating locations), PLR (based on three significant deteriorating locations), linear regression of MD and linear regression VFI over time.

visual field tests to the algorithm as input and will be able to see the output as a binary class, i.e., progressed or not progressed. They also will be able to observe the progression rate graphically.

From an algorithmic complexity perspective, progression detection using the optimization framework utilizes a sound mathematical framework with a single objective vector to create the progression detection environment while our previously described methods were two-step processes. Step one included unsupervised machine learning on cross-sectional visual fields (a separate dataset of visual field tests at the baseline visit) to find the glaucoma-associated clusters.

The glaucoma associated clusters were then decomposed into several axes (to identify optimal directions of progression) using independent or principal component analysis (step two). As can be inferred, our previously unsupervised machine learning-based approaches employ a more complex environment than the proposed approach for progression detection.

To compare the computational complexity of CDOF to the previous machine-learning-based approaches objectively, creating the progression detection environment using VIM [17] takes approximately 168 h (7 days) in a quad-core machine (eight gigabytes of memory), creating the GEM progression detection environment [21] takes approximately 3 h, while creating the proposed progression detection environment using the optimization framework takes a fraction of a minute using a similar machine. However, once the VIM and GEM progression detection environments have been established and criteria for progression detection have been defined, run-time is similar for VIM, GEM, and CDOF methods. CDOF retains an advantage of being modifiable in less time, because of the markedly reduced development time.

Comparing the computational complexity of all methods in order, linear regression of MD involves a single OLSR analysis and linear regression of VFI involves a combination of weighing the visual field points in conjunction with a single OLSR analysis. Therefore, linear regression of MD is the least computationally complex method followed by linear regression of VFI. CDOF involves a combination of visual field projection and a single OLSR analysis while VIM and GEM both involve a combination of visual field projection and seven OLSR analyses. PLR involves fifty-two OLSR analyses and PoPLR that involves fifty-two OLSR analyses on all permutations of visual field exams is the most computationally complex method.

Because CDOF is computationally and algorithmically less complex than previously described machine learning-based methods, VIM and GEM, according to Occam's razor principle [27], it is preferable (however, see below).

One possible limitation of our approach is the generation of 10-visit pseudo-longitudinal series from 5-visit visual field data in our stable group, tested over several weeks. This does not account for the effects of aging, glaucoma treatment, and long-term measurement variability observable over years.

Another possible limitation is that CDOF results in a single optimal direction for glaucoma progression, while we know the direction of progression is not limited to one. Even though this approach uses a single vector, its performance is not less effective than our previous approaches that used seven directions (VIM and GEM). However, unlike VIM and GEM, CDOF does not provide information about visible patterns of VF progression that could be useful to a clinician who is interested in the location of VF is progression in order to investigate the possibility of corresponding structural change (as corroborating evidence of disease-related progression). From the simplicity standpoint, approaches using linear regression of global indices provide a simpler and faster framework than other methods, with sensitivity for detecting known progression is greatly compromised.

Finally, it is possible that we have underestimated the performance of PoPLR. For PoPLR, at least seven independent exams are ideal to generate a robust outcome. Our stable dataset, with a mean of five exams, might affect the sensitivity of PoPLR, by increasing variability. For a more accurate comparison, we suggest using a dataset with at least seven longitudinal visual field exams. This limitation does not affect the comparison of progression detection performance of CDOF, VIM, GEM, PLR, MD, and VFI.

4. Conclusion

The proposed optimization framework provides a low complexity environment and is computationally more efficient than our previous approaches. Moreover, progression detection using optimization framework suggests a slightly higher sensitivity at higher specificities than VIM, GEM, PLR, and PoPLR methods and is as sensitive as VIM, GEM, PLR, and PoPLR at lower specificities. CDOF also is significantly more sensitive than methods based on linear regression of global indices provided by the standard instrument software. The proposed framework has potential application in glaucoma clinics for progression detection and could be applied to other longitudinal healthcare data to detect measurement change.

Grant support

NIH R01EY022039, NIH R01EY008208, NIH R01EY011008, NIH R01EY019869, P30EY022589, U10EY14267, NIH R01EY021818, an unrestricted grant from Research to Prevent Blindness (New York, NY), EyeSight Foundation of Alabama, Edith C. Blum Research Fund of the New York Glaucoma Research Institute, and participant incentive grants in the form of glaucoma medication at no cost from Alcon Laboratories, Allergan, Merck, and Pfizer.

Conflicts of interest

Siamak Yousefi: None.
Michael H. Goldbaum: None.
Ehsan S. Varnousfaderani: None.
Akram Belghith: None.
Tzyy-Ping Jung: None.
Felipe A. Medeiros: Alcon Laboratories (F), Allergan (F, C), Bausch & Lomb (F), Carl Zeiss Meditec (F, C), Heidelberg Engineering GmbH (F), Merck (F), Novartis (C), Sensimed (F), Topcon (F), Reichert (F).
Linda M. Zangwill: Carl Zeiss Meditec Inc. (F), Heidelberg Engineering GmbH (F, R), Optovue Inc. (F), Topcon Medical Systems Inc. (F).
Robert N. Weinreb: Alcon Laboratories Inc. (C), Allergan Inc. (C), Carl Zeiss Meditec Inc. (F, C), Heidelberg Engineering GmbH (F), Optovue Inc. (F), Topcon Medical Systems Inc. (F, C).
Christopher A. Girkin: None.
Jeffrey M. Liebmann: Alcon Laboratories Inc. (C), Allergan Inc. (C), Carl Zeiss Meditec Inc. (F), Diopsys Corp. (F, C), Heidelberg Engineering GmbH (F), Optovue Inc. (F, C), Pfizer Inc. (C), Topcon Medical Systems Inc. (F,C).
Christopher Bowd: None.

References

[1] R.N. Weinreb, T. Aung, F.A. Medeiros, The pathophysiology and treatment of glaucoma: a review, JAMA 311 (2014) 1901–1911.
[2] R.N. Weinreb, P.T. Khaw, Primary open-angle glaucoma, Lancet 363 (2004) 1711–1720.
[3] C.A. Johnson, P.A. Sample, G.A. Cioffi, J.R. Liebmann, R.N. Weinreb, Structure and function evaluation (SAFE): I. Criteria for glaucomatous visual field loss using standard automated perimetry (SAP) and short wavelength automated perimetry (SWAP), Am. J. Ophthalmol. 134 (2002) 177–185.
[4] A.P. Tanna, J.R. Bandi, D.L. Budenz, W.J. Feuer, R.M. Feldman, L.W. Herndon, et al., Interobserver agreement and intraobserver reproducibility of the subjective determination of glaucomatous visual field progression, Ophthalmology 118 (2011) 60–65.
[5] A.B. Ashraf, S. Gavenonis, D. Daye, C. Mies, M. Feldman, M. Rosen, et al., A multichannel Markov random field approach for automated segmentation of breast cancer tumor in DCE-MRI data using kinetic observation model, Med. Image Comput. Comput. Assist. Interv. 14 (2011) 546–553.
[6] B. Bengtsson, A. Heijl, A visual field index for calculation of glaucoma rate of progression, Am. J. Ophthalmol. 145 (2008) 343–353.
[7] J. Katz, D. Gilbert, H.A. Quigley, A. Sommer, Estimating progression of visual field loss in glaucoma, Ophthalmology 104 (1997) 1017–1025.
[8] F.W. Fitzke, R.A. Hitchings, D. Poinoosawmy, A.I. McNaught, D.P. Crabb, Analysis of visual field progression in glaucoma, Br. J. Ophthalmol. 80 (1996) 40–48.
[9] N. O'Leary, B.C. Chauhan, P.H. Artes, Visual field progression in glaucoma: estimating the overall significance of deterioration with permutation analyses of pointwise linear regression (PoPLR), Invest. Ophthalmol. Vis. Sci. 53 (2012) 6776–6784.
[10] H. Zhu, R.A. Russell, L.J. Saunders, S. Ceccon, D.F. Garway-Heath, D.P. Crabb, Detecting changes in retinal function: analysis with non-stationary Weibull error regression and spatial enhancement (ANSWERS), PLoS ONE 9 (2014).
[11] D. Bizios, A. Heijl, B. Bengtsson, Trained artificial neural network for glaucoma diagnosis using visual field data: a comparison with conventional algorithms, J. Glaucoma 16 (2007) 20–28.
[12] C. Bowd, I. Lee, M.H. Goldbaum, M. Balasubramanian, F.A. Medeiros, L.M. Zangwill, et al., Predicting glaucomatous progression in glaucoma suspect eyes using relevance vector machine classifiers for combined structural and functional measurements, Invest. Ophthalmol. Vis. Sci. 53 (2012) 2382–2389.
[13] Z. Burgansky-Eliash, G. Wollstein, T. Chu, J.D. Ramsey, C. Glymour, R.J. Noecker, et al., Optical coherence tomography machine learning classifiers for glaucoma detection: a preliminary study, Invest. Ophthalmol. Vis. Sci. 46 (2005) 4147–4152.
[14] S. Demirel, B. Fortune, J. Fan, R.A. Levine, R. Torres, H. Nguyen, et al., Predicting progressive glaucomatous optic neuropathy using baseline standard automated perimetry data, Invest. Ophthalmol. Vis. Sci. 50 (2009) 674–680.
[15] S. Yousefi, M.H. Goldbaum, M. Balasubramanian, T.P. Jung, R.N. Weinreb, F.A. Medeiros, et al., Glaucoma progression detection using structural retinal nerve fiber layer measurements and functional visual field points, IEEE Trans. Biomed. Eng. 61 (2014) 1143–1154.
[16] C. Bowd, R.N. Weinreb, M. Balasubramanian, I. Lee, G. Jang, S. Yousefi, et al., Glaucomatous patterns in Frequency Doubling Technology (FDT) perimetry data identified by unsupervised machine learning classifiers, PLoS ONE 9 (2014) e85941.
[17] M.H. Goldbaum, I. Lee, G. Jang, M. Balasubramanian, P.A. Sample, R.N. Weinreb, et al., Progression of patterns (POP): a machine classifier algorithm to identify glaucoma progression in visual fields, Invest. Ophthalmol. Vis. Sci. 53 (2012) 6557–6567.
[18] K. Chan, T.-W. Lee, T.J. Sejnowski, Variational Bayesian learning of ICA with missing data, Neural Comput. 15 (2003) 1991–2011 (2003/08/01).
[19] S. Yousefi, M.H. Goldbaum, L.M. Zangwill, F.A. Medeiros, C. Bowd, Recognizing patterns of visual field loss using unsupervised machine learning, Proc. SPIE 2014 (2014).

[20] B. Bengtsson, A. Heijl, A visual field index for calculation of glaucoma rate of progression, Am. J. Ophthalmol. 145 (2008) 343–353.
[21] S. Yousefi, M.H. Goldbaum, M. Balasubramanian, F.A. Medeiros, L.M. Zangwill, J.M. Liebmann, et al., Learning from data: recognizing glaucomatous defect patterns and detecting progression from visual field measurements, IEEE Trans. Biomed. Eng. 61 (2014) 2112–2124.
[22] N.M. Jansonius, On the accuracy of measuring rates of visual field change in glaucoma, Br. J. Ophthalmol. 94 (2010) 1404–1405.
[23] P. Åsman, A. Heijl, Glaucoma hemifield test: automated visual field evaluation, Arch. Ophthalmol. 110 (1992) 812–819.
[24] S. Boyd, L. Vandenberghe, Convex Optimization, Cambridge University Press, 2004.
[25] I. CVX Research, Matlab Software for Disciplined Convex Programming, Version 2.0, 2012.
[26] M.C. Grant, S.P. Boyd, Graph implementations for nonsmooth convex programs, in: Vincent D. Blondel, Stephen P. Boyd, Hidenori Kimura (Eds.), Recent Advances in Learning and Control, Springer-Verlag Limited, 2008, pp. 95–110.
[27] D. Nolan, Quantitative parsimony, Brit. J. Philos. Sci. 48 (1997) 329–343.